

# The universality of islands outside the horizon

Song He<sup>a,b,1</sup>, Yuan Sun<sup>a,2</sup>, Long Zhao<sup>a,c,d,3</sup>, Yu-Xuan Zhang<sup>a,4</sup>

<sup>a</sup>*Center for Theoretical Physics and College of Physics, Jilin University,  
Changchun 130012, People's Republic of China*

<sup>b</sup>*Max Planck Institute for Gravitational Physics (Albert Einstein Institute),  
Am Mühlenberg 1, 14476 Golm, Germany*

<sup>c</sup>*CAS Key Laboratory of Theoretical Physics, Institute of Theoretical Physics, Chinese  
Academy of Sciences, P.O. Box 2735, Beijing 100190, China*

<sup>d</sup>*School of Physics, University of Chinese Academy of Sciences, Beijing 100049, China*

## Abstract

We systematically calculate the quantum extremal surface (QES) associated with Hawking radiation for general  $D$ -dimensional ( $D \geq 2$ ) asymptotically flat (or AdS) eternal black holes using the island formula. By adopting the standard "black hole couples thermal baths" model, we find that a QES exists in the near-horizon region outside the black hole when  $c \cdot G_{(D)}$  is smaller enough where  $c$  is the central charge of the conformal matter and  $G_{(D)}$  the Newton constant. The locations of the QES in these backgrounds are obtained and the late-time radiation entropy saturates the two times of black hole entropy. Finally, we numerically check that the no island configuration exists once  $c \cdot G_{(D)}$  exceeds a certain upper bound in two-dimensional generalized dilaton theories (GDT).

---

<sup>1</sup>hesong@jlu.edu.cn

<sup>2</sup>sunyuan@jlu.edu.cn

<sup>3</sup>zhaolong@mail.itp.ac.cn

<sup>4</sup>yuxuanz18@mails.jlu.edu.cn

# Contents

<b>1</b>	<b>Introduction</b>	<b>1</b>
<b>2</b>	<b>Island formula in eternal black holes</b>	<b>3</b>
2.1	Setup and assumptions . . . . .	3
2.2	Without island, the radiation entropy diverges linearly . . . . .	5
2.3	Island emerges outside the horizon and saves the entropy bound . . . . .	5
2.4	Go beyond $c \cdot G_{(D)} \ll 1$ : Examples in two-dimensional dilaton gravity . . . . .	8
2.4.1	Eternal black holes in GDT . . . . .	9
2.4.2	Numerical results . . . . .	10
<b>3</b>	<b>Conclusions and prospect</b>	<b>14</b>
<b>A</b>	<b>Derivation of Eq.(19)</b>	<b>15</b>
<b>B</b>	<b>Derivation of Eq.(20)</b>	<b>17</b>
<b>C</b>	<b>Black hole thermodynamics in GDT</b>	<b>18</b>
<b>D</b>	<b>Models related by Weyl transformation</b>	<b>20</b>

## 1 Introduction

The black hole information paradox [1] is one of the most fundamental problems in quantum gravity. Resolving this problem has been regarded as the key to understanding quantum gravity. The black hole Hawking radiation behaves like thermal radiation implying that the entanglement entropy outside the black hole is monotonically increasing. On the other hand, quantum mechanics requires that the entanglement entropy of the radiation particles goes to zero at the end of the evaporation due to the evaporation process is unitary. In the AdS/CFT literature, there has been a new calculation of the fine-grained entropy of radiation for the evaporating black holes [2–6] and the time evolution of the fine-grained entropy satisfies the so-called Page curve [3, 4].

The holographic entanglement entropy was proposed from AdS/CFT correspondence [7, 8], and the corresponding quantum corrections to the entanglement entropy were investigated in [9, 10]. Then, the entanglement entropy can be calculated upto arbitrary orders by using notion of the QES [11]. The QES extremizes the generalized entropy which is the sum of area and bulk entanglement entropy. In terms of the prescription of minimal quantum extremal

surface [11], the fine-grained entanglement entropy of the Hawking radiation is proposed as [4]

$$S_{\text{Rad}}(A) = \min_I \left\{ \text{ext}_I \left[ \frac{\text{Area}(\partial I)}{4G_N} + S_{\text{matter}}(A \cup I) \right] \right\}, \quad (1)$$

where  $S_{\text{Rad}}$  is the generalized entropy and  $\text{Area}(\partial I)$  is the area of the boundary of island  $I$ . The entanglement entropy from matter part contains the UV divergence which is proportional to the island area, subject to a UV cut-off scale [12,13], and the Newton constant  $G_N$  must be renormalized [14]. The  $S_{\text{matter}}$  corresponds to the finite contribution of the matter entanglement entropy. This is the so called island formula. The island formula can be also derived from the replica trick for gravitational theories. From the gravitational path integral, the authors of [2,15] found that the replica wormholes can be regarded as saddle points exist in the island formula.

Initially, to realize the Page curve for the Hawking radiation process was implemented using the semiclassical theory of the two-dimensional black holes in the asymptotically AdS-JT (Jackiw-Teitelboim) gravity [2, 4, 16]. These studies indicated that islands will appear after the page time stage of the black hole evaporation and the location of island would be outside or inside the horizon. The islands reduce the entanglement entropy and makes Bekenstein-Hawking entropy [17–20] finite.

The research for page curve and island formula can be extended to many aspects, and a large amount of works have been done in this direction. For an incomplete list, for example higher dimensional black hole cases are considered in [21–27] as well as higher derivative gravity [28,29]. Also, the page curve for evaporating instead of external black holes are explored in [18,20,30–33]. Interestingly, the page curve can be realized in the moving mirror scenario [34–36], and other quantum information quantities except entanglement entropy are also investigated within island formula [37–43]. Meanwhile replica wormhole and double holography is an important framework in studying the page curve [44–47].

As pointed in [16], within the framework of the so-called "black hole couples thermal baths" model, the island appears outside the horizon for an external black hole in 2D JT gravity. The radiation entropy approaches  $2S_{BH}$  in the late time limit. There were several case-by-case studies, to confirm the above behavior of QES with the approximation that the central charge of thermal bath is greater than the inverse of Newton constant associated with a black hole. In this paper, we would like to systematically study QES for various 2D external black holes including asymptotically flat and AdS cases, and higher dimension cases. In these generic gravitational backgrounds, we try to extract universal features for the existence of QES and islands. We find that once the combination  $c \cdot G_{(D)}$  of central charge and Newton constant stays within a certain region, the QES and island configuration in such generic gravitational background always exists outside nearby the black hole event horizon, not inside the horizon. We further do the analytical and numerical self-consistency checks in several GDT.

The organization of this paper is as follows. In Section 2, we set up the generic "black

hole couples thermal baths" model and obtain certain constraints in terms of the existence of QES. To close this section, we do the numerically self-consistency checks and go beyond the  $c \cdot G_{(D)} \ll 1$  limit in 2D eternal black holes. The summary and prospect are given in section 3. Our conventions, useful formulae, and some calculation details are presented in the appendices.

## 2 Island formula in eternal black holes

### 2.1 Setup and assumptions

Let us consider a  $D$ -dimensional ( $D \geq 2$ ) gravitational system, which consists of a non-extremal asymptotically flat (or AdS) black hole and a thermal bath with which it reaches thermal equilibrium. The whole system is assumed to be filled with conformal matter with central charge  $c$ , and the black hole's metric is assumed under the Schwarzschild gauge as follows

$$ds^2 = -f(r)dt^2 + f(r)^{-1}dr^2 + r^2 d\Omega_{D-2}^2. \quad (2)$$

Here  $d\Omega_{D-2}^2$  is the unit metric on  $\mathbb{S}^{D-2}$ .  $f(r)$  is allowed to have multiple roots and  $r_h$  ( $f(r_h) = 0$ ) represents the largest one ( i.e., the location of the outermost horizon). The black hole's Hawking temperature and entropy are

$$T_H = \frac{\kappa}{2\pi} = \frac{f'(r_h)}{4\pi}, \quad S = \frac{A(r_h)}{4G_{(D)}}, \quad (3)$$

respectively. Thereinto,  $\kappa$  is surface gravity of the outermost horizon,  $G_{(D)}$  is  $D$ -dimensional Newton constant, and  $A(r)$  is a model-dependent function which stands for the area of the  $(D - 2)$ -sphere at radius  $r$  in  $D \geq 3$  dimensional Einstein gravity and represents the value of the dilaton field at  $r$  in two-dimensional dilaton gravity [48], etc.

The Penrose diagram of the full system might be depicted as Fig.1, and the coordinate transformations between Kruskal coordinates and Schwarzschild coordinates in the four wedges of the Penrose diagram of the black hole are set to following

$$\text{I: } \hat{u} = \kappa^{-1} e^{\kappa(t_R + r^*(r_R))}, \quad \hat{v} = -\kappa^{-1} e^{-\kappa(t_R - r^*(r_R))} \quad (r_R > r_h), \quad (4)$$

$$\text{II: } \hat{u} = \kappa^{-1} e^{\kappa(t_R + r^*(r_R))}, \quad \hat{v} = \kappa^{-1} e^{-\kappa(t_R - r^*(r_R))} \quad (r_R < r_h), \quad (5)$$

$$\text{III: } \hat{u} = -\kappa^{-1} e^{-\kappa(t_L - r^*(r_L))}, \quad \hat{v} = \kappa^{-1} e^{\kappa(t_L + r^*(r_L))} \quad (r_L > r_h), \quad (6)$$

$$\text{IV: } \hat{u} = -\kappa^{-1} e^{\kappa(t_L + r^*(r_L))}, \quad \hat{v} = -\kappa^{-1} e^{-\kappa(t_L - r^*(r_L))} \quad (r_L < r_h), \quad (7)$$

where  $r^* \equiv \int^r f(\tilde{r})^{-1} d\tilde{r}$  is tortoise coordinate. The transformations above give the length element in Kruskal coordinates

$$ds^2 = -e^{2\rho} d\hat{u}d\hat{v} + r_{R(L)}^2 d\Omega_{D-2}^2 \quad (e^{2\rho} \equiv f(r_{R(L)})e^{-2\kappa r^*(r_{R(L)})}). \quad (8)$$

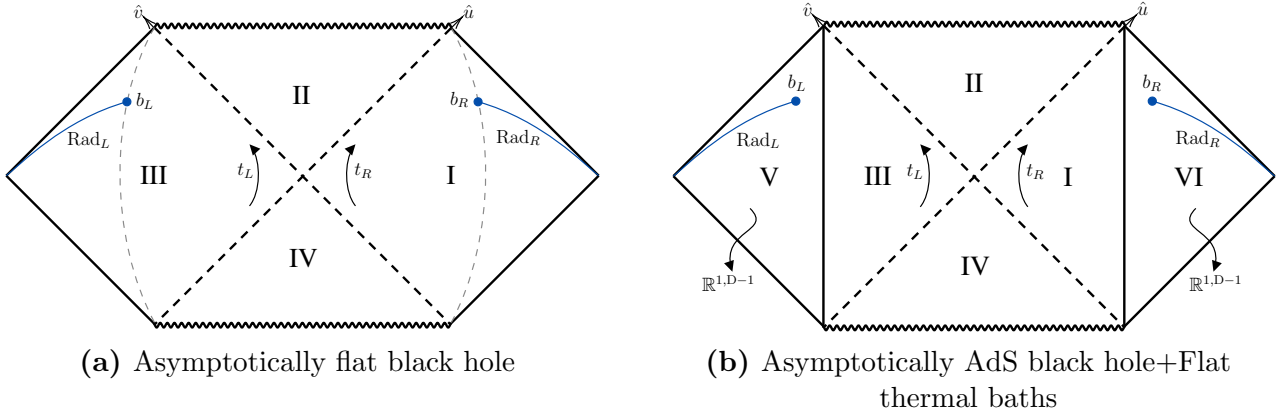


**Figure 1:** Penrose diagrams of the whole gravitational system (*Left:* Asymptotically flat black hole with single horizon and singularity. *right:* Asymptotically AdS black hole with single horizon and singularity). Each point on diagrams represents a  $(D - 2)$ -dimensional sphere. The dotted gray lines in (a) are boundaries of collecting region for the Hawking radiation. The blue lines stand for collecting region with boundaries  $b_{L(R)}$  in a schwarzschild time slice. We consider the symmetric case that  $t_{b_L} = t_{b_R} = t_b$  and  $r_{b_L}^* = r_{b_R}^* = r_b^*$ .

As shown in Fig.1, we have adopted the customary approach to deal with the black hole and the thermal bath: When spacetime is asymptotically flat, the region far away from the black hole is selected as the thermal bath [19, 20], and when spacetime is asymptotically AdS,  $D$ -dimensional flat spacetimes  $\mathbb{R}^{1,D-1}$  will be used as auxiliary thermal baths to be glued to both sides of the two-sided black hole [16]<sup>5</sup>.

It is also important to emphasize that, when  $D \geq 3$ , the  $s$ -wave approximation [22, 49] has been taken into account in the calculations of  $S_{\text{matter}}$  below. The entanglement entropy of matter between two shells  $S_1$  and  $S_2$  becomes

$$\begin{aligned}
 S_{\text{matter}}(S_1, S_2) &= \frac{c}{6} \log d^2(S_1, S_2) \\
 &= \frac{c}{6} \log \left| (\hat{u}(S_1) - \hat{u}(S_2)) (\hat{v}(S_1) - \hat{v}(S_2)) \sqrt{W(S_1)W(S_2)} \right|, \quad (9)
 \end{aligned}$$

when the quantum state of total system is vacuum in  $(\hat{u}, \hat{v})$  coordinates. In the above,  $W(S_1)$  and  $W(S_2)$  are warped factors of the metric at  $S_1$  and  $S_2$  under the  $(\hat{u}, \hat{v})$  coordinates, respectively.

<sup>5</sup>We follow the prescription in [16] but generalize it to higher-dimensions. Firstly the tortoise coordinates are normalized by requiring  $\lim_{r_{R(L)} \rightarrow \infty} r_{R(L)}^* = 0$ , such that the right (left) bath corresponds to  $r_{R(L)}^* > 0$ . The Kruskal coordinates thus can be extended to the baths (V and VI):

$$\begin{aligned}
 \text{V: } \quad \hat{u} &= -\kappa^{-1} e^{-\kappa(t_L - r_L^*)}, & \hat{v} &= \kappa^{-1} e^{\kappa(t_L + r_L^*)} & (r_L^* > 0), \\
 \text{VI: } \quad \hat{u} &= \kappa^{-1} e^{\kappa(t_R + r_R^*)}, & \hat{v} &= -\kappa^{-1} e^{-\kappa(t_R - r_R^*)} & (r_R^* > 0).
 \end{aligned}$$

Meanwhile, we assume that the two-sided black hole is truncated at  $r_R = \Lambda$  and  $r_L = \Lambda$  respectively, and the metric of the right (left) bath is set to following

$$ds^2 = f(\Lambda) \left( -dt_{R(L)}^2 + (dr_{R(L)}^*)^2 \right) + \left( \sqrt{f(\Lambda)} r_{R(L)}^* + \Lambda \right)^2 d\Omega_{D-2}^2$$

to ensure that two metrics (black hole and bath) are continuously connected at the cut-off. Note that this metric is flat.

## 2.2 Without island, the radiation entropy diverges linearly

In this section, we evaluate the entanglement entropy of the Hawking radiation at late times in the missing island construction. It shows that "information loss" is a common phenomenon for black holes we are considering.

Without island, the only contribution of (1) is coming from the collecting regions of the Hawking radiation (see  $\text{Rad}_L$  and  $\text{Rad}_R$  in Fig.1). The collecting region on the right (left) is the region outside the shell  $r_{R(L)}^* = r_{b_{R(L)}}^*$  in time slices of  $(t_{R(L)}, r_{R(L)}^*)$  coordinates and we shall choose the symmetric configuration  $r_{b_L}^* = r_{b_R}^* = r_b^*$  and  $t_{b_L} = t_{b_R} = t_b$  in the following calculations. Assuming that the state of total system is vacuum in  $(\hat{u}, \hat{v})$  coordinates, The formula can be further reduced to the entanglement entropy of the interval  $[b_L, b_R]$  by (9), that is

$$S_{\text{Rad}} = \frac{c}{6} \log \left| (\hat{u}(b_L) - \hat{u}(b_R)) (\hat{v}(b_L) - \hat{v}(b_R)) \sqrt{W(b_L)W(b_R)} \right|, \quad (10)$$

where

$$W(b_{R(L)}) = \begin{cases} -f(r_b)e^{-2\kappa r_b^*}, & \text{for asymptotically flat black holes,} \\ -f(\Lambda)e^{-2\kappa r_b^*}, & \text{for asymptotically AdS black holes.} \end{cases} \quad (11)$$

Simple calculation shows that

$$S_{\text{Rad}} = \begin{cases} \frac{c}{6} \log \left( 4\kappa^{-2} f(b) \cosh^2 \kappa t_b \right), & \text{for asymptotically flat black holes} \\ \frac{c}{6} \log \left( 4\kappa^{-2} f(\Lambda) \cosh^2 \kappa t_b \right), & \text{for asymptotically AdS black holes} \end{cases} \\ \simeq \frac{c}{3} \kappa t_b + \text{time independent terms.} \quad (12)$$

Notice that (12) holds for all black holes we are considering. The linear growth of radiation entropy when the island contribution is missing obviously contradicts the Page curve and thus leads to the information paradox for the black hole.

## 2.3 Island emerges outside the horizon and saves the entropy bound

In this section, we shall reconsider the entropy of the Hawking radiation by counting the contribution of the island. It is easy to verify that the equation determining the location of QES has no solution inside the horizon. Therefore the basic configuration is set as shown in Fig.2. As shown in Fig.2, we are continuing with the symmetric structure used in the previous section. The two boundaries of island are marked  $a_L$  and  $a_R$  respectively, and  $t_{a_L} = t_{a_R} = t_a$ ,  $r_{a_L} = r_{a_R} = r_a$ . After taking  $s$ -wave approximation for  $D \geq 3$ , it shows that the entanglement entropy of conformal matter in  $\{\text{Rad} \cup I\}$  can be well approximated by twice of the entanglement entropy in the single interval  $[a_R, b_R]$  when  $t_b$  and  $t_a \rightarrow \infty$  [50]

$$S_{\text{Rad}} = \frac{A(a_R)}{2G_{(D)}} + \frac{c}{3} \log \left| (\hat{u}(a_R) - \hat{u}(b_R)) (\hat{v}(a_R) - \hat{v}(b_R)) \sqrt{W(a_R)W(b_R)} \right|, \quad (13)$$

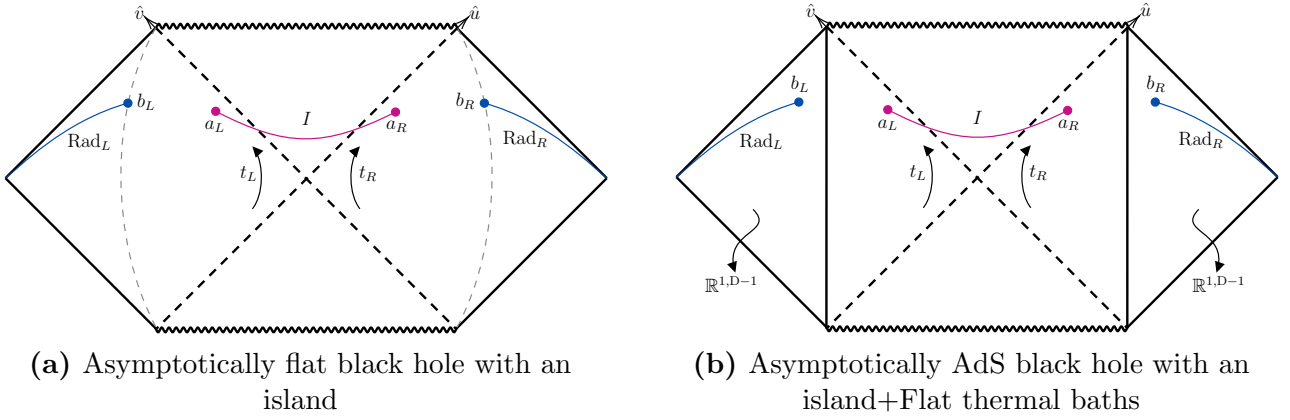


**Figure 2:** Penrose diagrams with islands (*Left:* Asymptotically flat black hole with single horizon and singularity. *right:* Asymptotically AdS black hole with single horizon and singularity). The pink lines are islands whose boundaries are outside the horizon. The dotted gray lines in (a) are boundaries of collecting region for the Hawking radiation. The blue lines stand for collecting region with boundaries  $b_{L(R)}$  in a Schwarzschild time slice. We consider the symmetric case that  $t_{b_L} = t_{b_R} = t_b$ ,  $t_{a_L} = t_{a_R} = t_a$ ,  $r_{a_L} = r_{a_R} = r_a$ ,  $r_{b_L}^* = r_{b_R}^* = r_b^*$ .

where  $W(a_R) = -f(r_a)e^{-2\kappa r_a^*}$  and  $W(b_R)$  is (11). Eq.(13) can be expressed in  $(t_R, r_R)$  coordinates

$$S_{\text{Rad}} = \frac{c}{3} \log \left| \kappa^{-2} (f(r_a)f(r_b)e^{-2\kappa(r_a^*+r_b^*)})^{\frac{1}{2}} \left( 2e^{\kappa(r_a^*+r_b^*)} \cosh[\kappa(t_b - t_a)] - (e^{2\kappa r_a^*} + e^{2\kappa r_b^*}) \right) \right| + \frac{A(r_a)}{2G_{(D)}}, \quad (14)$$

for asymptotically flat black holes.  $f(r_b) \rightarrow f(\Lambda)$  for asymptotically AdS black holes.

It's easy to find  $t_a$  should be equal to  $t_b$  when we extremise  $S_{\text{Rad}}$  with respect to  $t_a$ , then we arrive at a simpler expression compared to (14),

$$S_{\text{Rad}} = \frac{A(r_a)}{2G_{(D)}} + \frac{2c}{3} \log \left[ \frac{e^{\kappa r_b^*} - e^{\kappa r_a^*}}{\kappa} \right] + \frac{c}{6} \log \left[ f(r_a)f(r_b)e^{-2\kappa(r_a^*+r_b^*)} \right], \quad (15)$$

for asymptotically flat black holes.  $f(r_b) \rightarrow f(\Lambda)$  for asymptotically AdS black holes.

Taking partial derivative of  $S_{\text{Rad}}$  with respect to  $r_a$ , we meet the algebra equation of determining the location of QES ( $r_a$  here)

$$\partial_{r_a} S_{\text{Rad}} = \frac{A'(r_a)}{2G_{(D)}} - \frac{2c}{3} \frac{\kappa}{f(r_a) \left( e^{\kappa(r_b^*-r_a^*)} - 1 \right)} + \frac{c}{6} \frac{f'(r_a) - 2\kappa}{f(r_a)} = 0, \quad (16)$$

which is the same for both asymptotically flat black holes and asymptotically AdS black holes. There are some model-independent properties of the solution that can be extracted from (16), notwithstanding this algebra equation of  $r_a$  may be precisely solved only after  $f(r)$  and  $A(r)$  are given. The key point essentially comes from the fact that the near-horizon geometry is common to all non-extreme black holes. To show them clearly, let's rewrite (16) as follows

$$Y(r) \equiv \frac{3A'(r)}{2} \cdot \left( \frac{2e^{\kappa r^*}(r)}{f(r)} \left( \frac{\kappa}{e^{\kappa r_b^*} - e^{\kappa r^*(r)}} \right) + \frac{2\kappa - f'(r)}{2f(r)} \right)^{-1} = c \cdot G_{(D)}, \quad (17)$$

where the subscript  $a$  has been omitted for brevity. The zero points of  $\partial_{r_a} S_{\text{Rad}}$  now become the points of intersection between the horizontal line  $y = c \cdot G_{(D)}$  and the curve  $y = Y(r)$  ( $r_h < r < r_b$  for asymptotically flat and  $r_h < r < \Lambda$  for asymptotically AdS) on the  $r - y$  plane, as shown in Fig.4. Let's focus on the behavior of  $Y(r)$  near  $r_h$ . A rough estimation can be made since  $f(r) \approx 2\kappa(r - r_h)$  and  $r^*(r) \approx \frac{1}{2\kappa} \log \left[ \frac{r}{r_h} - 1 \right]$  for  $r \gtrsim r_h$ .  $Y(r)$  can thus be approximated to

$$Y(r) \approx \frac{3}{2} A'(r_h) \left( X \cdot r_h^{-1} e^{-\kappa r_b^*} \left( \frac{r}{r_h} - 1 \right)^{-\frac{1}{2}} - \frac{f''(r_h)}{4\kappa} \right)^{-1} \sim \sqrt{\frac{r}{r_h} - 1}, \quad (18)$$

where  $X$  is an undetermined constant. The approximate behavior of function  $Y$  near  $r_h$  is sufficient for us to draw two following conclusions:

**Conclusion 1.** *There must be a quantum extremal surface located in the near-horizon region outside the black hole,*

$$r_a = r_h + \frac{8\kappa(c \cdot G_{(D)})^2}{9A'(r_h)^2} \exp \left\{ -2\kappa r_b^* - 2\rho(r_h) \right\} + \mathcal{O} \left( (c \cdot G_{(D)})^3 \right), \quad (19)$$

when  $c \cdot G_{(D)} \ll 1$ .

**Conclusion 2.** *There has to be an upper bound on  $c \cdot G_{(D)}$  to have an island configuration.*

The second conclusion can be a direct corollary to the *boundedness theorem*, since  $Y(r)$  is a continuous function on the closed interval  $[r_h, r_b]$  ( $[r_h, \Lambda]$  for asymptotically AdS). While for the conclusion 1, firstly, the approximate behavior of  $Y$  guarantees that when  $c \cdot G_{(D)} \ll 1$  there must be a point of intersection near  $r_h$ , which is graphically obvious.<sup>6</sup> Secondly, the approximate formula (19) is obtained by Taylor expansion of the local inverse function of  $Y$  near  $r_h$ .<sup>7</sup> As listed in Table 1, we calculate the approximate locations of QESs for several common black holes by (19), which, in addition to coinciding with qualitative results in the literature [19], exactly matches the quantitative results in [22].<sup>8</sup>

Substituted the approximate solution (19) into (15), the late-time radiation entropy after including the island contribution can be obtained as<sup>9</sup>

$$\begin{aligned} S_{\text{Rad}}[\text{with island}] &= \frac{A(r_h)}{2G_{(D)}} + \frac{c}{3} \log d^2(r_h, r_b) - \frac{4\kappa c^2 G_{(D)}}{9A'(r_h)} \exp \left\{ -2\kappa r_b^* - 2\rho(r_h) \right\} + \mathcal{O}(c^3 G_{(D)}^2) \\ &= 2S_{\text{BH}} + \mathcal{O}(c) \quad (c \cdot G_{(D)} \ll 1). \end{aligned} \quad (20)$$

Note that the above approximation formula for the late-time radiation entropy also coincide with results in [22, 51]. Based on above results, we can reproduce the Page curve for generic

<sup>6</sup>One may worry that we may miss some other points of intersection. Indeed, for asymptotically flat black holes, it's not hard to find that there is another intersection near  $r_b$ , which we call  $r_{a'}$ . However, when considering the constraint that  $c \cdot G_{(D)} \ll 1$ , the leading order contribution of the island formula comes from the area term, and since  $r_{a'} > r_a$ , we have  $S_{\text{Rad}}(r_{a'}) > S_{\text{Rad}}(r_a)$ . The root near  $r_b$  is thus discarded.

<sup>7</sup>For details, please refer to Appendix A.

<sup>8</sup>In addition, Eq.(19) can also reproduce the results in [24,51] and differ by a scale factor from those of [23,52].

<sup>9</sup>Similar to (19), the derivation is a little tricky, please refer to Appendix B for details.



**Table 1:** Approximations of location of quantum extremal surface for several black holes

Black hole	$A(r)$	$f(r)$	$r_a - r_h \approx$
Witten(CGHS)	$e^{2\lambda r}$	$1 - e^{-2\lambda(r-r_h)}$	$\frac{2c^2 G_{(2)}^2}{9\lambda} \left( e^{2\lambda(r_h+r_b)} - e^{4\lambda r_h} \right)^{-1}$
JT	$\frac{r}{L}$	$\frac{r^2 - r_h^2}{L^2}$	$\frac{2c^2 G_{(2)}^2 L^2}{9r_h} e^{-2\frac{r_h}{L^2} r_b^*}$
BTZ	$2\pi r$	$\frac{r^2 - r_h^2}{L^2}$	$\frac{c^2 G_{(3)}^2}{18\pi^2 r_h} e^{-2\frac{r_h}{L^2} r_b^*}$
4d-Schwarzschild	$4\pi r^2$	$1 - \frac{r_h}{r}$	$\frac{c^2 G_{(4)}^2}{144\pi^2 r_h^2 (r_b - r_h)} e^{1 - \frac{r_b}{r_h}}$
4d-non-extremal RN	$4\pi r^2$	$\left(1 - \frac{r_+}{r}\right) \left(1 - \frac{r_-}{r}\right)$	$\frac{c^2 G_{(4)}^2}{144\pi^2 r_+^2 (r_b - r_+)} \left(\frac{r_b - r_-}{r_+ - r_-}\right)^{\frac{r_-}{r_+}} e^{-\frac{(r_b - r_+)(r_+ - r_-)}{r_+^2}}$

non-extremal spherically symmetric black holes as Fig.3. Under the constraint  $c \cdot G_{(D)} \ll 1$ , the estimation of the Page time also has a concise and uniform form,  $t_{\text{Page}} \sim \frac{6S_{\text{BH}}}{c\kappa} = \frac{3S_{\text{BH}}}{\pi c T_{\text{H}}}$  for all black holes that meet the requirements. Note that, as shown in the next section, once the condition  $c \cdot G_{(D)} \ll 1$  is broken, the late-time radiation entropy after considering the island contribution does not saturate near  $2S_{\text{BH}}$ , but has a significant deviation. This suggests that the estimation for the Page time will also change.

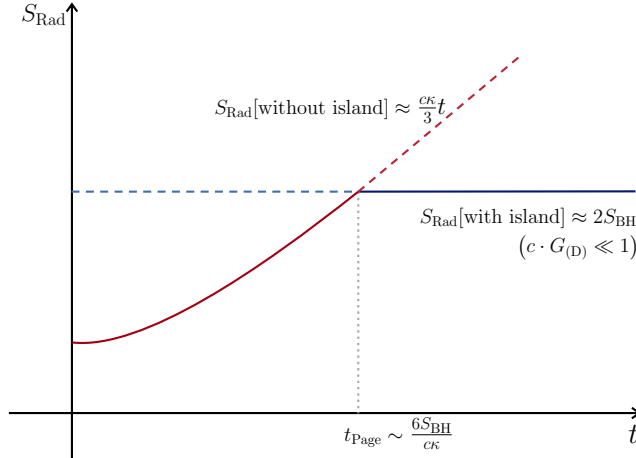


**Figure 3:** The Page curve for  $D$ -dimensional non-extremal spherically symmetric black holes. When the contribution of the island is not considered, the late-time radiation entropy increases linearly (red dashed line); After considering the island's contribution and the condition  $c \cdot G_{(D)} \ll 1$ , the late-time radiation entropy is approximately saturated at  $2S_{\text{BH}}$  (blue solid line).

## 2.4 Go beyond $c \cdot G_{(D)} \ll 1$ : Examples in two-dimensional dilaton gravity

In the previous section, we show that when  $c \cdot G_{(D)} \ll 1$ , there must be a QES located in the near-horizon region outside the black hole, and the late-time radiation entropy given by it is saturated near  $2S_{\text{BH}}$  (with sub-leading corrections of order  $c$ ). It is natural to ask how does

the island change when  $c \cdot G_{(D)} \ll 1$  is no longer satisfied. One can expect that the location of the QES might be model-dependent and the late-time radiation entropy may deviate from  $2S_{\text{BH}}$  significantly. In this section, we shall numerically solve the equation (16) in eternal black hole solutions of two-dimensional GDT to look at the change of the island as  $c \cdot G_{(2)}$  varies.

### 2.4.1 Eternal black holes in GDT

The action of the GDT in 2 dimensions is given by [48]

$$I_{\text{GDT}} = \frac{1}{16\pi G_{(2)}} \int_{\mathcal{M}} \sqrt{-g} (\phi R + U(\phi) (\nabla\phi)^2 + V(\phi)) d^2x + \frac{1}{8\pi G_{(2)}} \int_{\partial\mathcal{M}} \sqrt{-h} (\phi K - \mathcal{L}_{\text{c.t.}}) dx. \quad (21)$$

Note that in the above equation,  $U(\phi)$  and  $V(\phi)$  are arbitrary functions of dilaton field  $\phi$ . The boundary term in the action involving the extrinsic curvature  $K$  and a counterterm  $\mathcal{L}_{\text{c.t.}}$ <sup>10</sup> plays two main roles [54]: 1) It makes the variational properties of the action compatible with the semi-classical approximation of the path integral. 2) It renders the Euclidean on-shell action finite and gives the correct black hole thermodynamics.

Given proper functions  $U$  and  $V$ , one can in principle obtain a series of physically reasonable solutions. Notably, a family of eternal black hole solutions have been given in [48, 54]: Under the Schwarzschild gauge of the metric and the time-independent presupposition of the dilaton field

$$ds^2 = -f(r)dt^2 + f(r)^{-1}dr^2, \quad \phi = \phi(r), \quad (22)$$

the equations of motion corresponding to (21)

$$\partial_\phi U(\phi) (\nabla\phi)^2 + 2U(\phi) \nabla^2\phi - \partial_\phi V(\phi) = R, \quad (23)$$

$$U \nabla_a \phi \nabla_b \phi - \nabla_a \nabla_b \phi + g_{ab} \left[ \nabla^2\phi - \frac{1}{2}U(\phi) (\nabla\phi)^2 - \frac{1}{2}V(\phi) \right] = 0 \quad (24)$$

can be solved as

$$r = \int^\phi e^{Q(\phi')} d\phi' + C, \quad (25)$$

$$f(r) \equiv F(\phi(r)) = (W(\phi) - 16\pi G_{(2)}M) e^{Q(\phi)}, \quad (26)$$

where

$$Q(\phi) = Q_0 - \int^\phi U(\phi') d\phi', \quad (27)$$

$$W(\phi) = W_0 + \int^\phi V(\phi') e^{Q(\phi')} d\phi'. \quad (28)$$

---

<sup>10</sup>The exact form of  $\mathcal{L}_{\text{c.t.}}$  depends on the selection of  $U(\phi)$  and  $V(\phi)$ , please refer to Appendix C for details. One can also refer to [53] for details.

Here  $C$ ,  $Q_0$ ,  $W_0$  are integration constants and  $M$  is the mass parameter<sup>11</sup> of the black hole as shown in appendix C to preserve the thermodynamic relation with the black hole temperature  $T$  and entropy  $S$ ,

$$T = \beta^{-1} = \frac{f'(r_h)}{4\pi} = \frac{\partial_\phi W}{4\pi} \Big|_{\phi_h} \quad (\phi_h \equiv \phi(r_h)), \quad (29)$$

$$S = \frac{\phi_h}{4G_{(2)}}, \quad (30)$$

where  $r_h$  means the location of the outermost horizon.

## 2.4.2 Numerical results

To show the behavior of the QES and its corresponding late-time radiation entropy with respect to  $c \cdot G_{(2)}$ , we mainly focus on the following concrete cases: (Weyl-related) Witten (or CGHS) black hole [55–57], (Weyl-related) Schwarzschild black hole [58], (Weyl-related) black hole attractor [59], JT black hole [60, 61], and AdS-Schwarzschild black hole [62, 63]. The first six black holes are (asymptotically) flat<sup>12</sup> and the prefix "Weyl-related" means that the metric of the theory is related to the original theory by a Weyl transformation (see Appendix D). The metrics, dilaton profiles and corresponding  $U$ ,  $V$  functions are summarized in Table 2.

**Table 2:** Serval eternal black hole solutions in two-dimensional GDT.

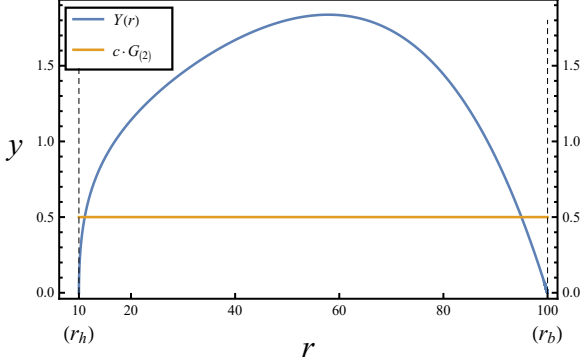
Black hole	$U(\phi)$	$V(\phi)$	$\phi(r)$	$f(r)$
Witten (CGHS)	$\phi^{-1}$	$4\lambda^2\phi$	$e^{2\lambda r}$	$1 - e^{-2\lambda(r-r_h)}$
Weyl-related Witten (CGHS)	0	$4\lambda^2$	$2\lambda r$	$2\lambda(r - r_h)$
Schwarzschild	$(2\phi)^{-1}$	$2\lambda^2$	$\lambda^2 r^2$	$1 - \frac{r_h}{r}$
Weyl-related Schwarzschild	0	$2\lambda^2\phi^{-\frac{1}{2}}$	$2\lambda r$	$\sqrt{2\lambda r} - \sqrt{2\lambda r_h}$
Black hole attractor	0	$4\lambda^2\phi^{-1}$	$2\lambda r$	$\log \frac{r}{r_h}$
Weyl-related black hole attractor	$\phi^{-1}$	$4\lambda^2$	$e^{2\lambda r}$	$2\lambda e^{-2\lambda r}(r - r_h)$
JT	0	$\frac{2}{L^2}\phi$	$\frac{r}{L}$	$\frac{r^2 - r_h^2}{L^2 r}$
AdS-Schwarzschild	$(2\phi)^{-1}$	$2\lambda^2 + \frac{6}{L^2}\phi$	$\lambda^2 r^2$	$\frac{(r-r_h)(r^2+r_h r+r_h^2+L^2)}{L^2 r}$

We first draw  $Y$ -functions (17) for black holes mentioned above. As demonstrated in Fig.4, for (asymptotically) flat black holes,  $Y(r)$  is a concave function that is continuous and consis-

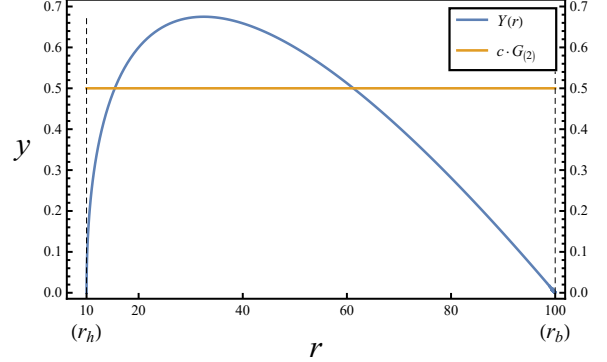
<sup>11</sup> $M$  is also the conserved charge associated with the Killing vector  $\partial_t$  and coincides with the ADM mass if  $\lim_{\phi \rightarrow \infty} W(\phi)e^{Q(\phi)} = 1$ .

<sup>12</sup>The curvature for the Weyl-related Witten (CGHS) black hole is zero.

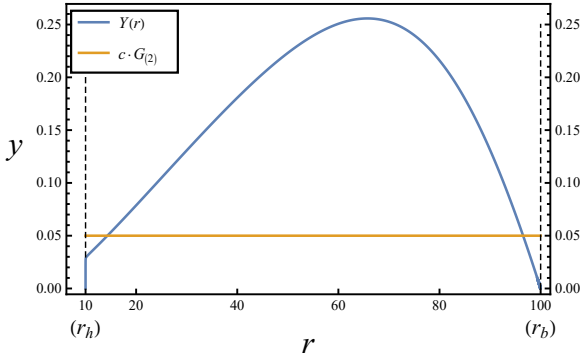
tently greater than or equals to 0 on the closed interval  $[r_h, r_b]$  (0 is evaluated at two endpoints). This indicates that when  $0 < c \cdot G_{(2)} < \max_{r_h < r < r_b} [Y(r)]$ , there must be two roots, one is closer to the horizon (denoted as  $a$ ) and the other is closer to the boundary of the collecting region (denoted as  $a'$ ). By comparing the late-time radiation entropy given by the two roots, as shown in Fig.5,  $a'$  is discarded due to the larger entropy given. When  $c \cdot G_{(2)} = \max_{r_h < r < r_b} [Y(r)]$ ,  $a$  coincides with  $a'$ . When  $c \cdot G_{(2)} > \max_{r_h < r < r_b} [Y(r)]$ , Eq.(16) has no solution and the island structure is thus destroyed, as stated in conclusion 2.



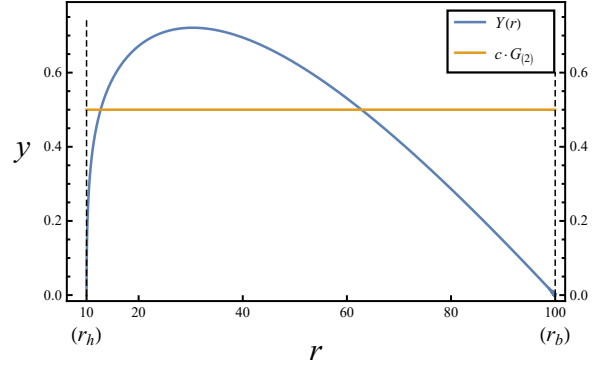
(a)  $Y(r)$  for Witten (CGHS) black hole



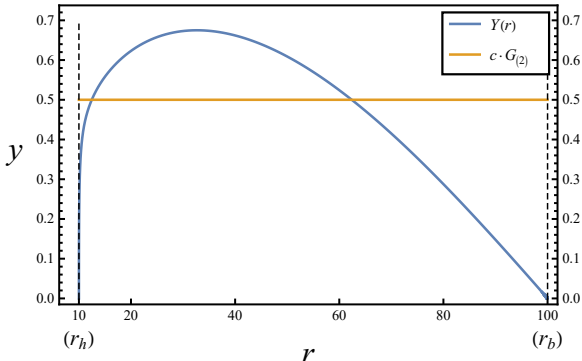
(b)  $Y(r)$  for Weyl-related Witten (CGHS) black hole



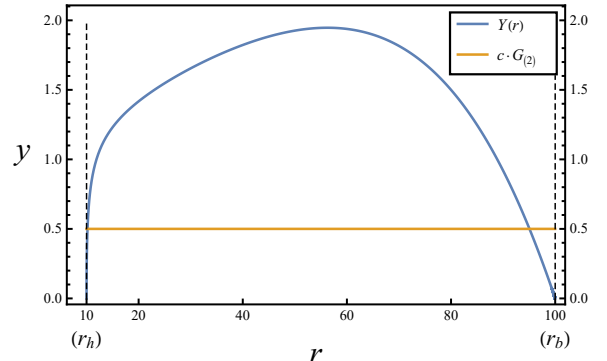
(c)  $Y(r)$  for Schwarzschild black hole



(d)  $Y(r)$  for Weyl-related Schwarzschild black hole



(e)  $Y(r)$  for black hole attractor



(f)  $Y(r)$  for Weyl-related black hole attractor

**Figure 4:**  $Y$ -functions (17) for (asymptotically) flat black holes. We draw these diagrams by setting  $r_h = 10$ ,  $\lambda = 10^{-2}$ ,  $r_b = 10r_h$ ,

The situation will be changed for (asymptotically) AdS black holes. As shown in Fig.6,

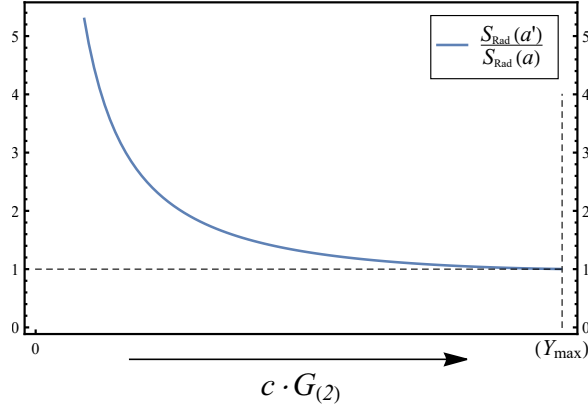
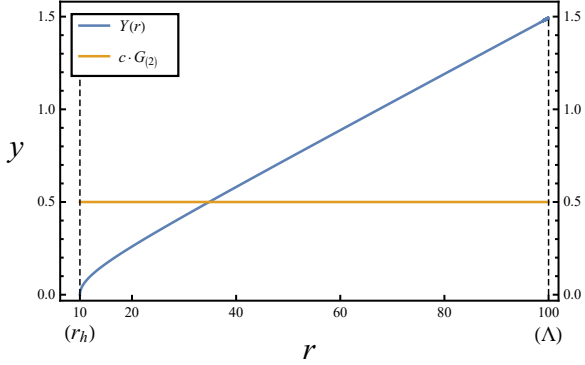
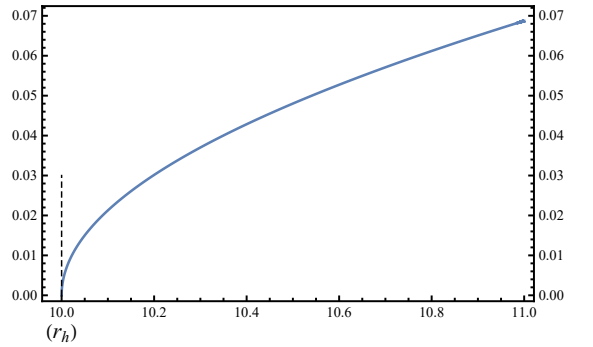


**Figure 5:** The ratio of the late-time radiation entropy given by the two roots of (16) for (asymptotically) flat black holes.  $a$  represents the root near  $r_h$  and  $a'$  represents the root near  $r_b$ . The numerical result shows that the root near the horizon will always be the boundary of island, if there is one.

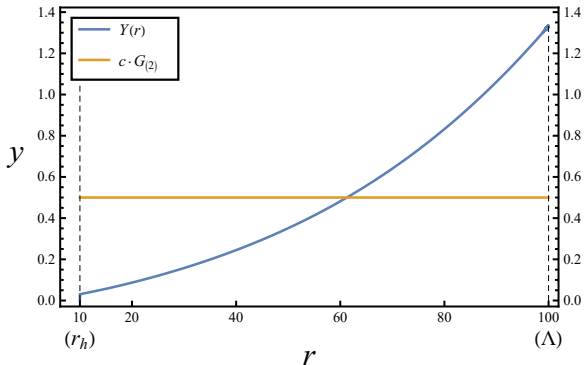
$Y(r)$  is monotonically increasing from zero on the interval  $[r_h, \Lambda]$ , which indicates that eq.(16) has one and only one root if and only if  $0 < c \cdot G_{(2)} \leq Y(\Lambda)$ . Therefore, as stated in conclusion 2, for (asymptotically) AdS black holes,  $c \cdot G_{(2)}$  has an upper bound after the truncation is given. For JT and AdS-Schwarzschild black holes this is given by the value of  $Y(r)$  at cut-off. It can be seen that no matter it is asymptotic flat (Fig.4) or asymptotic AdS (Fig.6(b),(d)),



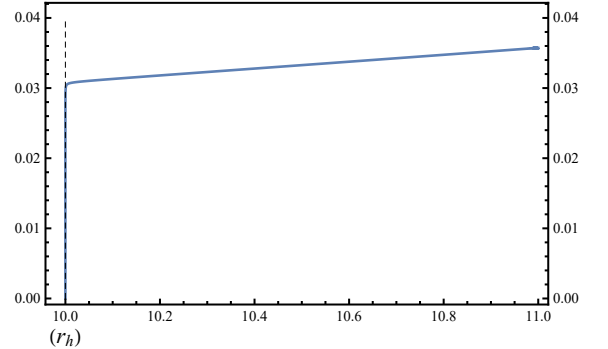
(a)  $Y(r)$  for JT black hole



(b) Enlarged view of Fig.6(a) at  $r_h$



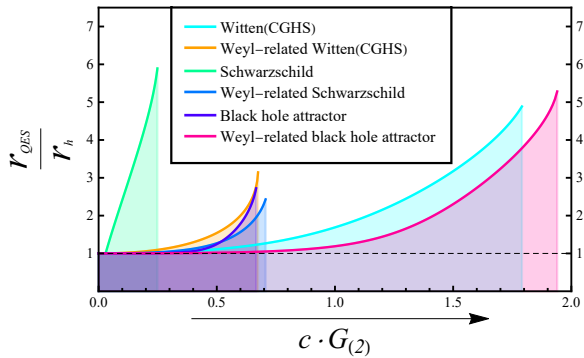
(c)  $Y(r)$  for AdS-Schwarzschild black hole



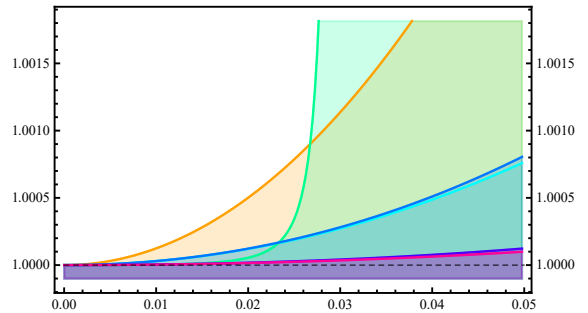
(d) Enlarged view of Fig.6(c) at  $r_h$

**Figure 6:**  $Y$ -functions (17) for (asymptotically) AdS black holes. We draw these diagrams by setting  $r_h = 10$ ,  $L = 100$ ,  $r_b^* = 0$ ,  $\Lambda = 10r_h$  ( $\lambda = 10^{-2}$  for AdS-Schwarzschild).

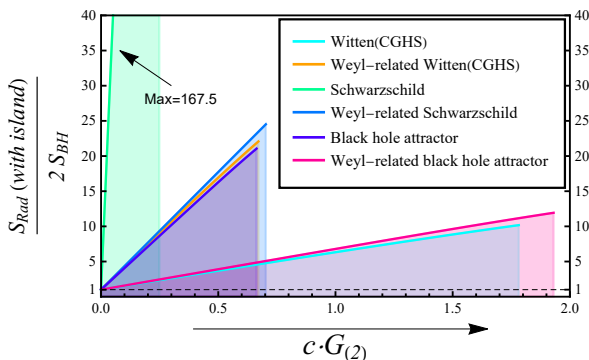
the behavior of  $Y$ -function near  $r_h$  is similar to that of the square root function  $\sqrt{\frac{r}{r_h} - 1}$ , which is consistent with the previous analysis.



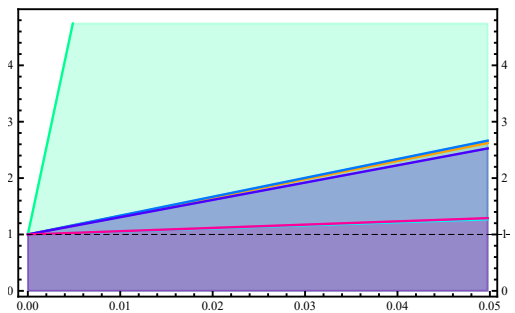
(a)  $r_{\text{QES}}/r_h$  for asymptotically flat black holes



(b) Enlarged view of Fig.7(a) at  $c \cdot G_{(2)} \sim 0$



(c)  $S_{\text{Rad}}/2S_{\text{BH}}$  for asymptotically flat black holes

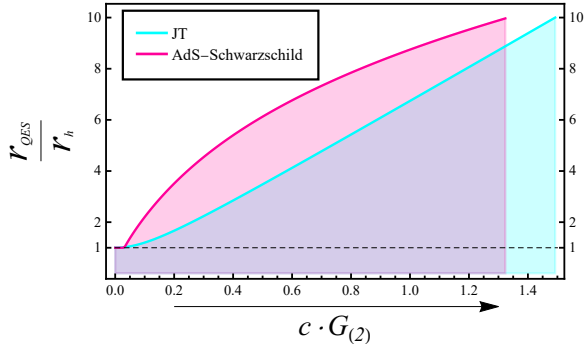


(d) Enlarged view of Fig.7(c) at  $c \cdot G_{(2)} \sim 0$

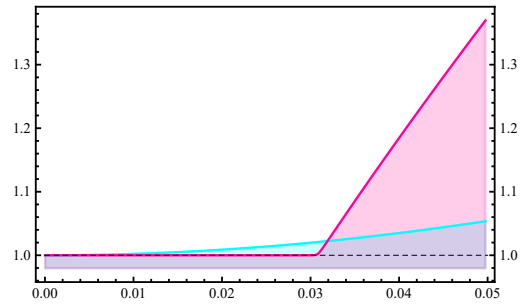
**Figure 7:** Curves of the QESs and their corresponding late-time radiation entropy with respect to  $c \cdot G_{(2)}$  (for asymptotically flat black holes). Diagrams are plotted with setting  $r_h = 10$ ,  $\lambda = 10^{-2}$ ,  $r_b = 10r_h$ ,  $G_{(2)} = 1/8\pi$ .

By solving the intersection of  $y = Y(r)$  and  $y = c \cdot G_{(2)}$  numerically, we obtain a series of curves of  $r_{\text{QES}}$  with respect to  $c \cdot G_{(2)}$ , see Fig.7(a),(b) for (asymptotically) flat black holes and Fig.8(a),(b) for (asymptotically) AdS black holes. The corresponding late-time radiation entropy for (asymptotically) flat and AdS black holes are plotted as Fig.7(c),(d) and Fig.8(c),(d) respectively.

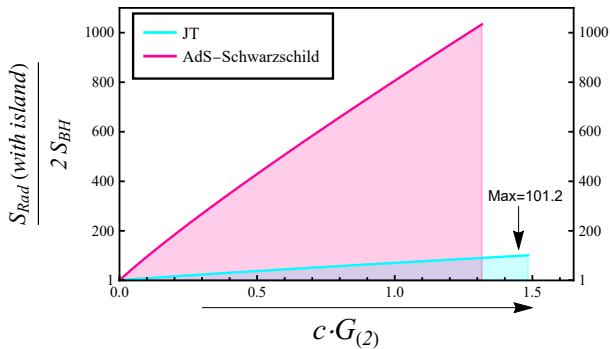
According to the results in Fig.7 and 8, we can summarize the behavior of the quantum extremum surface and its corresponding late-time radiation entropy with respect to  $c \cdot G_{(2)}$ : When  $c \cdot G_{(2)} \ll 1$  (or  $c \cdot G_{(2)} \sim 0$ ), the location of the QES and the late-time radiation entropy are described by (19) and (20) respectively. It results in the QES located in the near-horizon region of the black hole and is a square function of  $c \cdot G_{(2)}$ , and the radiation entropy is approximately equal to two times the black hole entropy and is a linear function of  $c$ . When  $c \cdot G_{(2)}$  gradually increases, the QES will gradually move away from the horizon, and the radiation entropy will obviously deviate from the black-hole entropy. When  $c \cdot G_{(2)}$  grows beyond a certain limit, assuming that  $r_b$  (or the cut-off  $\Lambda$  for asymptotically AdS black holes) has been fixed, the equation governing the location of the QES (16) will have no solution and the island configuration will be destroyed.



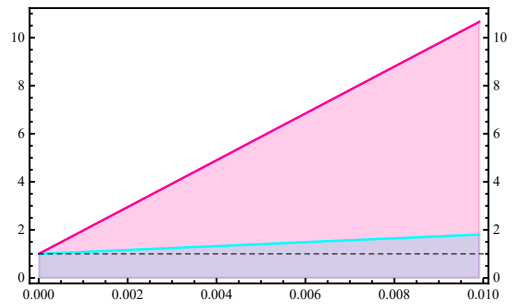
(a)  $r_{\text{QES}}/r_h$  for asymptotically AdS black holes



(b) Enlarged view of Fig.8(a) at  $c \cdot G_{(2)} \sim 0$



(c)  $S_{\text{Rad}}/2S_{\text{BH}}$  for AdS black holes



(d) Enlarged view of Fig.8(c) at  $c \cdot G_{(2)} \sim 0$

**Figure 8:** Curves of the QESs and their corresponding late-time radiation entropy with respect to  $c \cdot G_{(2)}$  (for AdS black holes). Diagrams are plotted with setting  $r_h = 10$ ,  $L = 100$ ,  $r_b^* = 0$ ,  $\Lambda = 10r_h$ ,  $G_{(2)} = 1/8\pi$  ( $\lambda = 10^{-2}$  for the AdS-Schwarzschild black hole).

### 3 Conclusions and prospect

In this paper, we systematically study the QES associated with the Hawking radiation for general  $D$ -dimensional ( $D \geq 2$ ) asymptotically flat (or AdS) eternal black holes using the island formula. We focus on the non-extremal black hole with spherical symmetry. In this case, the near-horizon geometry is common to all non-extreme black holes and we can use the s-wave approximation in higher dimensional ( $D \geq 3$ ) calculating of the matter field entropy. We have obtained the following conclusions:

- When  $c \cdot G_{(D)} \ll 1$ , thanks to the common near horizon structure, there must be a quantum extremal surface (QES) located in the near-horizon region outside the black hole,

$$r_{\text{QES}} = r_h + \frac{8\kappa(c \cdot G_{(D)})^2}{9A'(r_h)^2} \exp \left\{ -2\kappa r_b^* - 2\rho(r_h) \right\} + \mathcal{O}((c \cdot G_{(D)})^3), \quad (31)$$

and the late time radiation entropy saturates  $2S_{\text{BH}}$ . The formula (31) is compatible with various known results in [19, 22–24, 51, 52] and the late time behaviour of the radiation entropy is in good agreement with the previous studies [2–6].

- We go beyond the  $c \cdot G_{(D)} \ll 1$  limit and scan the parameter space numerically to analyze

the location of the QES and its corresponding radiation entropy. It can be shown generally by the boundedness theorem that there must be an upper bound on  $c \cdot G_{(D)}$  to have an island configuration. Besides, the numerical results manifest that the location of the QES is just out of the event horizon when  $c \cdot G_{(D)} \ll 1$ . As the value of  $c \cdot G_{(D)}$  increases, the QES gradually goes away from the black hole event horizon and the radiation entropy bound will obviously deviate from  $2S_{\text{BH}}$ .

It will be interesting to extend our analysis to the near extremal black hole and black hole without spherical symmetry, such as the planar or axisymmetric black hole. Another thing to reconsider is the gravitational effects of the bath in the asymptotically flat black hole because the thermal bath in this case is a gravitational system intrinsically. In asymptotically AdS couple to a gravitating bath, one finds that there is a new saddle point of the bulk geometry in the replica calculation, namely a wormhole connecting the black hole and the gravitational bath [64]. After the Page time, this configuration is the dominant contribution and this phenomenon can be regarded as a realization of ER=EPR [65]. The most interesting future problem is to see how an island is generated dynamically after the page time during the black hole evaporation process. To our knowledge, one can qualitatively reproduce the page curve behavior in several asymptotically flat (or AdS) eternal black holes. However, they can not tell how the black hole information is restored in a concrete way. We are ignorant of the details of the black hole evaporation process even in the semi-classical level. To dynamically generate the island will be an important aspect to reveal the mystery of the black hole information paradox.

## Acknowledgements

We would like to thank Miao He, Shan-Ming Ruan, and Hao Ouyang for the helpful discussion. S.H. would like to appreciate the financial support from Jilin University, Max Planck Partner group as well as Natural Science Foundation of China Grants (No.12075101, No.1204756). Y.S. is supported by the National Natural Science Foundation of China Grants (No.12105113).

## A Derivation of Eq.(19)

In this appendix, we present the details of the derivation of (19). The key is to find the second derivative of the local inverse of  $Y$  around  $r_h$  (the first derivative is zero), which can be expressed in terms of the derivative of the primitive function

$$(Y^{-1})'' \Big|_{Y(r_h)} = - \frac{Y''}{(Y')^3} \Big|_{r_h}. \quad (32)$$

Firstly, it's useful to set  $Y = \frac{3}{2}A'Z^{-1}$ , and thereinto,

$$Z \equiv \alpha\beta + \gamma, \quad \alpha \equiv \frac{2e^{\kappa r^*(r)}}{f}, \quad \beta \equiv \frac{\kappa}{e^{\kappa r_b^*} - e^{\kappa r^*(r)}}, \quad \gamma \equiv \frac{2\kappa - f'}{2f}. \quad (33)$$



$Z$  is blow up when  $r \rightarrow r_h$ , as is evident from the following limits

$$\lim_{r \rightarrow r_h} \alpha \sim \lim_{r \rightarrow r_h} \frac{1}{\sqrt{\frac{r}{r_h} - 1}} = \infty, \quad \lim_{r \rightarrow r_h} \beta = \kappa e^{-\kappa r_b^*} \equiv \beta_h, \quad \lim_{r \rightarrow r_h} \gamma = \frac{-f''(r_h)}{f'(r_h)} \equiv \gamma_h. \quad (34)$$

Let's write down the derivative of  $Y$

$$Y' = \frac{3}{2} A'' Z^{-1} - \frac{3}{2} A' \frac{Z'}{Z^2}, \quad Y'' = \frac{3}{2} A''' Z^{-1} - 3A'' \frac{Z'}{Z^2} - \frac{3}{2} A' \left( \frac{Z''}{Z^2} - 2 \frac{(Z')^2}{Z^3} \right), \quad (35)$$

where

$$\begin{aligned} Z' &= \alpha' \beta + \alpha \beta' + \gamma' \\ &= \alpha f^{-1} \beta (\kappa - f') + \alpha^2 \frac{\beta^2}{2} + f^{-1} \left( -\frac{f''}{2} - \gamma f' \right), \end{aligned} \quad (36)$$

and

$$\begin{aligned} Z'' &= \alpha'' \beta + 2\alpha' \beta' + \alpha \beta'' + \gamma'' \\ &= \alpha f^{-2} \beta (\kappa - f') (\kappa - 2f') - \alpha f^{-1} \beta f'' + \alpha^2 f^{-1} \beta^2 (\kappa - f') \\ &\quad + \alpha^2 f^{-1} \beta^2 \frac{(\kappa - f')}{2} + \alpha^3 \frac{\beta^3}{2} + f^{-2} (f' f'' + 2\gamma (f')^2) - f^{-1} \left( \frac{1}{2} f''' + \gamma f'' \right). \end{aligned} \quad (37)$$

In the above we have used the derivatives of  $\alpha$ ,  $\beta$ , and  $\gamma$  up to the second-order

$$\alpha' = \alpha f^{-1} (\kappa - f'), \quad \alpha'' = \alpha f^{-2} (\kappa - f') (\kappa - 2f') - \alpha f^{-1} f'', \quad (38)$$

$$\beta' = \alpha \frac{\beta^2}{2}, \quad \beta'' = \alpha f^{-1} \beta^2 \frac{(\kappa - f')}{2} + \alpha^2 \frac{\beta^3}{2}, \quad (39)$$

$$\gamma' = f^{-1} \left( -\frac{f''}{2} - \gamma f' \right), \quad \gamma'' = f^{-2} (f' f'' + 2\gamma (f')^2) - f^{-1} \left( \frac{1}{2} f''' + \gamma f'' \right). \quad (40)$$

According to (36-37) and the limits of  $\alpha$ ,  $\beta$ , and  $\gamma$ , we have

$$\frac{Z'}{Z^2} = \frac{e^{-\kappa r^*(r)}}{2} \cdot \frac{\beta (\kappa - f') + \mathcal{O}(\alpha^{-1})}{\beta^2 + \mathcal{O}(\alpha^{-1})}, \quad (41)$$

$$\frac{Z''}{Z^2} = \frac{e^{-\kappa r^*(r)}}{2f} \cdot \frac{\beta (\kappa - f') (\kappa - 2f') + \mathcal{O}(\alpha^{-1})}{\beta^2 + \mathcal{O}(\alpha^{-1})}, \quad (42)$$

$$\frac{(Z')^2}{Z^3} = \frac{e^{-\kappa r^*(r)}}{2f} \cdot \frac{\beta^2 (\kappa - f')^2 + \mathcal{O}(\alpha^{-1})}{\beta^3 + \mathcal{O}(\alpha^{-1})}, \quad (43)$$

which leads to the following two limits

$$\begin{aligned} &\lim_{r \rightarrow r_h} f e^{\kappa r^*(r)} Y''(r) \\ &= -\frac{3}{2} A'(r_h) \lim_{r \rightarrow r_h} \left( \frac{1}{2} \cdot \frac{\beta (\kappa - f') (\kappa - 2f') + \mathcal{O}(\alpha^{-1})}{\beta^2 + \mathcal{O}(\alpha^{-1})} - \frac{\beta^2 (\kappa - f')^2 + \mathcal{O}(\alpha^{-1})}{\beta^3 + \mathcal{O}(\alpha^{-1})} \right) \\ &= -\frac{3\kappa^2 A'(r_h)}{4\beta_h}, \end{aligned} \quad (44)$$

$$\begin{aligned} &\lim_{r \rightarrow r_h} f e^{\kappa r^*(r)} (Y')^3 \\ &= \frac{-3^3}{2^6} (A'(r_h))^3 \lim_{r \rightarrow r_h} f e^{-2\kappa r^*(r)} \cdot \frac{\beta^3 (\kappa - f')^3 + \mathcal{O}(\alpha^{-1})}{\beta^6 + \mathcal{O}(\alpha^{-1})} \\ &= \frac{3^3 \kappa^3}{4^3} (A'(r_h))^3 e^{2\rho(r_h)} \beta_h^{-3}. \end{aligned} \quad (45)$$

The second derivative of the local inverse of  $Y$  at  $r_h$  can thus be obtained by using above limits

$$(Y^{-1})'' \Big|_{Y(r_h)} = \lim_{r \rightarrow r_h} \frac{-Y''}{(Y')^3} = \kappa \left( \frac{3}{4} A'(r_h) \exp \{ \rho(r_h) + \kappa r_b^* \} \right)^{-2}. \quad (46)$$

In the light of the Taylor expansion of  $Y(r)^{-1}$  at  $Y(r_h) = 0$ , we finally arrive at the approximation of  $r_a$  upto the second-order of  $c^2 G_{(D)}^2$

$$\begin{aligned} r_a &= r_h + \frac{1}{2} (Y^{-1})'' \Big|_{Y(r_h)} \cdot (c \cdot G_{(D)})^2 + \mathcal{O} \left( (c \cdot G_{(D)})^3 \right) \\ &= r_h + \frac{8\kappa (c \cdot G_{(D)})^2}{9A'(r_h)^2} \exp \left\{ -2\kappa r_b^* - 2\rho(r_h) \right\} + \mathcal{O} \left( (c \cdot G_{(D)})^3 \right). \end{aligned} \quad (47)$$

## B Derivation of Eq.(20)

In this appendix, we demonstrate the derivation of (20). Firstly (15) is essentially

$$S_{\text{Rad}}(r) = \frac{A(r)}{2G_{(D)}} + \frac{c}{3} \log d^2(r, r_b) \quad (t = t_b), \quad (48)$$

where the first term is the area term, which is easy to evaluate according to (19)

$$\begin{aligned} \frac{A(r_a)}{2G_{(D)}} &= \frac{A(r_h)}{2G_{(D)}} + \frac{A'(r_h)}{2G_{(D)}} (r_a - r_h) + \mathcal{O}((r_a - r_h)^2) \\ &= \frac{A(r_h)}{2G_{(D)}} + \frac{4\kappa c^2 \cdot G_{(D)}}{9A'(r_h)} \exp \left\{ -2\kappa r_b^* - 2\rho(r_h) \right\} + \mathcal{O}(c^3 G_{(D)}^2). \end{aligned} \quad (49)$$

We then focus on the matter term. Since the approximate behavior of  $Y$  near  $r_h$  is (18), meanwhile  $Y(r) = -\frac{3}{2} A'(r) (\partial_r \log d^2(r, r_b))^{-1}$ , which gives that the approximate behavior of  $\log d^2(r, r_b)$  near  $r_h$  is  $C_h - \sqrt{\frac{r}{r_h} - 1}$ , where  $C_h \equiv \log d^2(r_h, r_b)$ . We can thus obtain its approximation by Taylor expansion of its local inverse function at  $r_h$

$$r = r_h + \frac{1}{2} \left( (\log d^2(r, r_b))^{-1} \right)'' \Big|_{r_h} \cdot \left( \log d^2(r, r_b) - C_h \right)^2. \quad (50)$$

The key step again becomes finding the second derivative of the inverse function at  $r_h$

$$\left( (\log d^2(r, r_b))^{-1} \right)'' = -\frac{(\log d^2(r, r_b))''}{\left( (\log d^2(r, r_b))' \right)^3} = -\frac{Z'}{Z^3}, \quad (51)$$

where  $Z$  is defined as (33). In terms of the limits obtained in Appendix A, it's not difficult to find that

$$\begin{aligned} \lim_{r \rightarrow r_h} \left( (\log d^2(r, r_b))^{-1} \right)'' &= \lim_{r \rightarrow r_h} \left( \frac{f e^{-2\kappa r^*}}{4} \cdot \frac{\beta(f' - \kappa) + \mathcal{O}(\alpha^{-1})}{\beta^3 + \mathcal{O}(\alpha^{-1})} \right) \\ &= \frac{1}{4\kappa} \exp \{ 2\kappa r_b^* + 2\rho(r_h) \}. \end{aligned} \quad (52)$$

We then inversely solve for the approximation of  $\log d^2(r_a, r_b)$  based on (50) and (52)

$$\begin{aligned}\log d^2(r_a, r_b) &\approx C_h - \sqrt{\frac{2(r_a - r_h)}{\left(\left(\log d^2(r, r_b)\right)^{-1}\right)''\Big|_{r_h}}} \\ &= C_h - \frac{8\kappa c \cdot G_{(D)}}{3A'(r_h)} \exp\{-2\kappa r_b^* - 2\rho(r_h)\}.\end{aligned}\quad (53)$$

Combine (49) with (53), the final answer arrives

$$\begin{aligned}S_{\text{Rad}}(\text{with island}) &= \frac{A(r_a)}{2G_{(D)}} + \frac{c}{3} \log d^2(r_a, r_b) \\ &\approx \frac{A(r_h)}{2G_{(D)}} + \frac{c}{3} \log d^2(r_h, r_b) - \frac{4\kappa c^2 \cdot G_{(D)}}{9A'(r_h)} \exp\{-2\kappa r_b^* - 2\rho(r_h)\} + \mathcal{O}(c^3 G_{(D)}^2).\end{aligned}\quad (54)$$

## C Black hole thermodynamics in GDT

In this appendix, we derive the thermodynamic quantities for the 2d dilaton gravity models with action (21).<sup>13</sup> We start with the corresponding Euclidean version

$$\begin{aligned}I_E &= -\frac{1}{16\pi G_{(2)}} \int_{\mathcal{M}} \sqrt{g} (\phi R + U(\phi) (\nabla\phi)^2 + V(\phi)) d^2x \\ &\quad - \frac{1}{8\pi G_{(2)}} \int_{\partial\mathcal{M}} \sqrt{h} \phi K dx + \frac{1}{8\pi G_{(2)}} \int_{\partial\mathcal{M}} \sqrt{h} \mathcal{L}_{\text{c.t.}} dx,\end{aligned}\quad (55)$$

where  $\mathcal{M}$  is spacetime region outside the black hole and the corresponding boundary  $\partial\mathcal{M}$  is  $\{r = r_h\} \cup \{r = r_{\text{reg.}}\}$ . Note that  $r_{\text{reg.}}$  is a regulator and should be removed by taking the limit  $r_{\text{reg.}} \rightarrow \infty$ .

The boundary counterterm  $\mathcal{L}_{\text{c.t.}}$ , as we will see below, should be of form

$$\mathcal{L}_{\text{c.t.}} = \sqrt{W(\phi)e^{-Q(\phi)}},\quad (56)$$

where the definitions of  $W(\phi)$  and  $Q(\phi)$  are (28) and (27), respectively. We show this point by reproducing the correct thermodynamics of the black hole.

We start with evaluating the Euclidean action for the black hole solution (25–26). The bulk

---

<sup>13</sup>Certain assumptions have been made, 1)  $\lim_{r \rightarrow +\infty} \phi = +\infty$ . 2)  $\lim_{\phi \rightarrow +\infty} W(\phi) = +\infty$ . 3)  $e^Q \neq 0$  for finite  $\phi$ , in this derivation.

contribution reads

$$\begin{aligned}
I_E^{\text{bulk}} &= \frac{-1}{16\pi G_{(2)}} \int_{\mathcal{M}} \sqrt{g} \left\{ \phi R + U(\phi) (\nabla\phi)^2 + V(\phi) \right\} d^2x \\
&= \frac{-1}{16\pi G_{(2)}} \int_0^\beta d\tau \int_{r_h}^{r_{\text{reg.}}} dr \left\{ -\phi f''(r) + U(\phi) f(r) \left( \frac{d\phi}{dr} \right)^2 + V(\phi) \right\} \\
&= \frac{-\beta}{16\pi G_{(2)}} \int_{\phi_h}^{\phi_{\text{reg.}}} d\phi \left\{ -\phi \partial_\phi^2 W + \phi U \partial_\phi W + \phi W \partial_\phi U - 16\pi G_{(2)} M \phi \partial_\phi U \right. \\
&\quad \left. + U(W - 16\pi G_{(2)} M) + \partial_\phi W \right\} \\
&= \frac{-\beta}{16\pi G_{(2)}} \left\{ -\phi \partial_\phi W \Big|_{\phi_h}^{\phi_{\text{reg.}}} + 2W \Big|_{\phi_h}^{\phi_{\text{reg.}}} + \phi_{\text{reg.}} U(\phi_{\text{reg.}}) (W(\phi_{\text{reg.}}) - 16\pi G_{(2)} M) \right\}. \tag{57}
\end{aligned}$$

Let us next consider the on-shell Gibbons-Hawking-York(GHY) term

$$\begin{aligned}
I_E^{\text{GHY}} &= -\frac{1}{8\pi G_{(2)}} \int_{\partial\mathcal{M}} \sqrt{h} \phi K dx \\
&= -\frac{\beta}{8\pi G_{(2)}} \sqrt{f(r_{\text{reg.}})} \cdot \phi_{\text{reg.}} K(r_{\text{reg.}}) \\
&= \frac{-\beta}{16\pi G_{(2)}} \left\{ \phi_{\text{reg.}} \partial_\phi W(\phi_{\text{reg.}}) - \phi_{\text{reg.}} U(\phi_{\text{reg.}}) (W(\phi_{\text{reg.}}) - 16\pi G_{(2)} M) \right\}. \tag{58}
\end{aligned}$$

It's clear to see that the on-shell bulk term plus the on-shell GHY term equals

$$\frac{\beta}{16\pi G_{(2)}} \left\{ 2W(\phi_h) - 2W(\phi_{\text{reg.}}) - \phi_h \partial_\phi W(\phi_h) \right\}. \tag{59}$$

The above equation is divergent when  $r_{\text{reg.}} \rightarrow \infty$  since we have assumed that  $\lim_{\phi \rightarrow \infty} W(\phi) = \infty$ .

The final contribution in (55) is the boundary counterterm

$$\begin{aligned}
I_E^{\text{c.t.}} &= \frac{1}{8\pi G_{(2)}} \int_{\partial\mathcal{M}} \sqrt{h} \mathcal{L}_{\text{c.t.}} dx \\
&= \frac{\beta}{8\pi G_{(2)}} \sqrt{(W(\phi_{\text{reg.}}) - 16\pi G_{(2)} M) e^{Q(\phi_{\text{reg.}})}} \cdot \sqrt{W(\phi_{\text{reg.}}) e^{-Q(\phi_{\text{reg.}})}} \\
&= \frac{\beta}{8\pi G_{(2)}} \left\{ W(\phi_{\text{reg.}}) - 8\pi G_{(2)} M + \mathcal{O}(W(\phi_{\text{reg.}})^{-1}) \right\}. \tag{60}
\end{aligned}$$

Summing over above contribution and letting  $\phi_{\text{reg.}} \rightarrow \infty$ , the total on-shell action reads

$$I_E^{\text{total}} = \beta M - S, \tag{61}$$

where we have used the definitions of black hole temperature (29) and Wald entropy (30). The free energy of black hole in the canonical ensemble reads

$$\mathcal{F} = -\frac{1}{\beta} \log \mathcal{Z} \sim -\frac{1}{\beta} \log e^{-I_E^{\text{total}}} = M - TS. \tag{62}$$

## D Models related by Weyl transformation

An intriguing feature of the 2d-dilaton gravity model is that one can eliminate (or recover) the kinetic term of the dilaton in the original theory by applying a Weyl transformation [66–68]. Let's consider a new metric  $\hat{g}_{\mu\nu}$  related to  $g_{\mu\nu}$  by

$$g_{\mu\nu} = e^{-2\Omega} \hat{g}_{\mu\nu}, \quad \Omega = \frac{1}{2} \int^{\phi} U(\phi') d\phi'. \quad (63)$$

The bulk term of (21) can be re-expressed as follows in terms of  $\hat{g}$

$$\begin{aligned} \int_{\mathcal{M}} \sqrt{-g} (\phi R + U(\phi) (\nabla\phi)^2 + V(\phi)) d^2x &= \int_{\mathcal{M}} \sqrt{-\hat{g}} (\phi \hat{R} + e^{-2\Omega} V(\phi)) d^2x \\ &+ \int_{\partial\mathcal{M}} \sqrt{-\hat{h}} \phi U(\phi) \hat{n}^\mu \hat{\nabla}_\mu \phi dx, \end{aligned} \quad (64)$$

where  $\hat{R}$  and  $\hat{\nabla}$  are Ricci scalar and covariant derivative corresponding to  $\hat{g}_{\mu\nu}$ ,  $\hat{n}^\mu$  is the unit vector normal to  $\partial\mathcal{M}$ . Ignoring the boundary term of no interest, we arrive a simpler theory with vanished kinetic term of dilaton. Three things are noteworthy about the new theory (64): 1) It gives a linear dilaton solution, i.e.,  $\phi_{\text{new}}(r) = e^{-Q_0 r}$ . 2) The new metric solution is closely related to the original one. We have  $f_{\text{new}}(r) \equiv F_{\text{new}}(\phi_{\text{new}}) = e^{-2\Omega} F|_{\phi=\phi_{\text{new}}}$ , where  $F(\phi)$  is solution of the original theory. 3) The black hole thermodynamic quantities are invariant under the Weyl transformation.<sup>14</sup>

## References

- [1] S. W. Hawking, *Breakdown of Predictability in Gravitational Collapse*, *Phys. Rev. D* **14** (1976) 2460–2473.
- [2] A. Almheiri, T. Hartman, J. Maldacena, E. Shaghoulian and A. Tajdini, *Replica Wormholes and the Entropy of Hawking Radiation*, *JHEP* **05** (2020) 013, [1911.12333].
- [3] G. Penington, *Entanglement Wedge Reconstruction and the Information Paradox*, *JHEP* **09** (2020) 002, [1905.08255].
- [4] A. Almheiri, R. Mahajan, J. Maldacena and Y. Zhao, *The Page curve of Hawking radiation from semiclassical geometry*, *JHEP* **03** (2020) 149, [1908.10996].
- [5] A. Almheiri, T. Hartman, J. Maldacena, E. Shaghoulian and A. Tajdini, *The entropy of Hawking radiation*, *Rev. Mod. Phys.* **93** (2021) 035002, [2006.06872].
- [6] A. Almheiri, N. Engelhardt, D. Marolf and H. Maxfield, *The entropy of bulk quantum fields and the entanglement wedge of an evaporating black hole*, *JHEP* **12** (2019) 063, [1905.08762].

---

<sup>14</sup>The reason comes from the following observation:  $W(\phi)$  is invariant under the transformation (63).

- [7] S. Ryu and T. Takayanagi, *Holographic derivation of entanglement entropy from AdS/CFT*, *Phys. Rev. Lett.* **96** (2006) 181602, [hep-th/0603001].
- [8] V. E. Hubeny, M. Rangamani and T. Takayanagi, *A Covariant holographic entanglement entropy proposal*, *JHEP* **07** (2007) 062, [0705.0016].
- [9] T. Barrella, X. Dong, S. A. Hartnoll and V. L. Martin, *Holographic entanglement beyond classical gravity*, *JHEP* **09** (2013) 109, [1306.4682].
- [10] T. Faulkner, A. Lewkowycz and J. Maldacena, *Quantum corrections to holographic entanglement entropy*, *JHEP* **11** (2013) 074, [1307.2892].
- [11] N. Engelhardt and A. C. Wall, *Quantum Extremal Surfaces: Holographic Entanglement Entropy beyond the Classical Regime*, *JHEP* **01** (2015) 073, [1408.3203].
- [12] L. Bombelli, R. K. Koul, J. Lee and R. D. Sorkin, *A Quantum Source of Entropy for Black Holes*, *Phys. Rev. D* **34** (1986) 373–383.
- [13] M. Srednicki, *Entropy and area*, *Phys. Rev. Lett.* **71** (1993) 666–669, [hep-th/9303048].
- [14] L. Susskind and J. Uglum, *Black hole entropy in canonical quantum gravity and superstring theory*, *Phys. Rev. D* **50** (1994) 2700–2711, [hep-th/9401070].
- [15] G. Penington, S. H. Shenker, D. Stanford and Z. Yang, *Replica wormholes and the black hole interior*, 1911.11977.
- [16] A. Almheiri, R. Mahajan and J. Maldacena, *Islands outside the horizon*, 1910.11077.
- [17] H. Z. Chen, Z. Fisher, J. Hernandez, R. C. Myers and S.-M. Ruan, *Information Flow in Black Hole Evaporation*, *JHEP* **03** (2020) 152, [1911.03402].
- [18] T. J. Hollowood and S. P. Kumar, *Islands and Page Curves for Evaporating Black Holes in JT Gravity*, *JHEP* **08** (2020) 094, [2004.14944].
- [19] T. Anegawa and N. Iizuka, *Notes on islands in asymptotically flat 2d dilaton black holes*, *JHEP* **07** (2020) 036, [2004.01601].
- [20] F. F. Gautason, L. Schneiderbauer, W. Sybesma and L. Thorlacius, *Page Curve for an Evaporating Black Hole*, *JHEP* **05** (2020) 091, [2004.00598].
- [21] A. Almheiri, R. Mahajan and J. E. Santos, *Entanglement islands in higher dimensions*, *SciPost Phys.* **9** (2020) 001, [1911.09666].
- [22] K. Hashimoto, N. Iizuka and Y. Matsuo, *Islands in Schwarzschild black holes*, *JHEP* **06** (2020) 085, [2004.05863].

- [23] X. Wang, R. Li and J. Wang, *Islands and Page curves of Reissner-Nordström black holes*, *JHEP* **04** (2021) 103, [2101.06867].
- [24] M.-H. Yu and X.-H. Ge, *Page Curves and Islands in Charged Dilaton Black Holes*, 2107.03031.
- [25] B. Ahn, S.-E. Bak, H.-S. Jeong, K.-Y. Kim and Y.-W. Sun, *Islands in charged linear dilaton black holes*, 2107.07444.
- [26] G. K. Karananas, A. Kehagias and J. Taskas, *Islands in linear dilaton black holes*, *JHEP* **03** (2021) 253, [2101.00024].
- [27] Y. Lu and J. Lin, *Islands in Kaluza-Klein black holes*, 2106.07845.
- [28] M. Alishahiha, A. Faraji Astaneh and A. Naseh, *Island in the presence of higher derivative terms*, *JHEP* **02** (2021) 035, [2005.08715].
- [29] J. Hernandez, R. C. Myers and S.-M. Ruan, *Quantum extremal islands made easy. Part III. Complexity on the brane*, *JHEP* **02** (2021) 173, [2010.16398].
- [30] T. Hartman, E. Shaghoulian and A. Strominger, *Islands in Asymptotically Flat 2D Gravity*, *JHEP* **07** (2020) 022, [2004.13857].
- [31] K. Goto, T. Hartman and A. Tajdini, *Replica wormholes for an evaporating 2D black hole*, *JHEP* **04** (2021) 289, [2011.09043].
- [32] H. Z. Chen, Z. Fisher, J. Hernandez, R. C. Myers and S.-M. Ruan, *Evaporating Black Holes Coupled to a Thermal Bath*, *JHEP* **01** (2021) 065, [2007.11658].
- [33] X. Wang, R. Li and J. Wang, *Page curves for a family of exactly solvable evaporating black holes*, *Phys. Rev. D* **103** (2021) 126026, [2104.00224].
- [34] I. Akal, Y. Kusuki, N. Shiba, T. Takayanagi and Z. Wei, *Entanglement Entropy in a Holographic Moving Mirror and the Page Curve*, *Phys. Rev. Lett.* **126** (2021) 061604, [2011.12005].
- [35] I. A. Reyes, *Moving Mirrors, Page Curves, and Bulk Entropies in AdS<sub>2</sub>*, *Phys. Rev. Lett.* **127** (2021) 051602, [2103.01230].
- [36] I. Akal, Y. Kusuki, N. Shiba, T. Takayanagi and Z. Wei, *Holographic moving mirrors*, 2106.11179.
- [37] K. Kawabata, T. Nishioka, Y. Okuyama and K. Watanabe, *Probing Hawking radiation through capacity of entanglement*, *JHEP* **05** (2021) 062, [2102.02425].

- [38] J. Kumar Basak, D. Basu, V. Malvimat, H. Parihar and G. Sengupta, *Islands for Entanglement Negativity*, 2012.03983.
- [39] S. Choudhury, S. Chowdhury, N. Gupta, A. Mishara, S. P. Selvam, S. Panda et al., *Circuit Complexity From Cosmological Islands*, *Symmetry* **13** (2021) 1301, [2012.10234].
- [40] Y. Ling, P. Liu, Y. Liu, C. Niu, Z.-Y. Xian and C.-Y. Zhang, *Reflected Entropy in Double Holography*, 2109.09243.
- [41] T. Li, M.-K. Yuan and Y. Zhou, *Defect Extremal Surface for Reflected Entropy*, 2108.08544.
- [42] V. Chandrasekaran, M. Miyaji and P. Rath, *Including contributions from entanglement islands to the reflected entropy*, *Phys. Rev. D* **102** (2020) 086009, [2006.10754].
- [43] K. Kawabata, T. Nishioka, Y. Okuyama and K. Watanabe, *Replica wormholes and capacity of entanglement*, 2105.08396.
- [44] H. Geng and A. Karch, *Massive islands*, *JHEP* **09** (2020) 121, [2006.02438].
- [45] E. Caceres, A. Kundu, A. K. Patra and S. Shashi, *Warped Information and Entanglement Islands in AdS/WCFT*, *JHEP* **07** (2021) 004, [2012.05425].
- [46] H. Geng, Y. Nomura and H.-Y. Sun, *Information paradox and its resolution in de Sitter holography*, *Phys. Rev. D* **103** (2021) 126004, [2103.07477].
- [47] H. Geng, S. Lüst, R. K. Mishra and D. Wakeham, *Holographic BCFTs and Communicating Black Holes*, *jhep* **08** (2021) 003, [2104.07039].
- [48] D. Grumiller, W. Kummer and D. V. Vassilevich, *Dilaton gravity in two-dimensions*, *Phys. Rept.* **369** (2002) 327–430, [hep-th/0204253].
- [49] S. Hemming and E. Keski-Vakkuri, *Hawking radiation from AdS black holes*, *Phys. Rev. D* **64** (2001) 044006, [gr-qc/0005115].
- [50] H. Casini, C. D. Fosco and M. Huerta, *Entanglement and alpha entropies for a massive Dirac field in two dimensions*, *J. Stat. Mech.* **0507** (2005) P07007, [cond-mat/0505563].
- [51] C. H. Nam, *Entanglement entropy and Page curve of black holes with island in massive gravity*, 2108.10144.
- [52] W. Kim and M. Nam, *Entanglement entropy of asymptotically flat non-extremal and extremal black holes with an island*, *Eur. Phys. J. C* **81** (2021) 869, [2103.16163].



- [53] R.-G. Cai, S. He, S.-J. Wang and Y.-X. Zhang, *Revisit on holographic complexity in two-dimensional gravity*, *JHEP* **08** (2020) 102, [2001.11626].
- [54] D. Grumiller and R. McNees, *Thermodynamics of black holes in two (and higher) dimensions*, *JHEP* **04** (2007) 074, [hep-th/0703230].
- [55] G. Mandal, A. M. Sengupta and S. R. Wadia, *Classical solutions of two-dimensional string theory*, *Mod. Phys. Lett. A* **6** (1991) 1685–1692.
- [56] E. Witten, *On string theory and black holes*, *Phys. Rev. D* **44** (1991) 314–324.
- [57] C. G. Callan, Jr., S. B. Giddings, J. A. Harvey and A. Strominger, *Evanescent black holes*, *Phys. Rev. D* **45** (1992) R1005, [hep-th/9111056].
- [58] K. Schwarzschild, *On the gravitational field of a mass point according to Einstein's theory*, *Sitzungsber. Preuss. Akad. Wiss. Berlin (Math. Phys. )* **1916** (1916) 189–196, [physics/9905030].
- [59] D. Grumiller, *Long time black hole evaporation with bounded Hawking flux*, *JCAP* **05** (2004) 005, [gr-qc/0307005].
- [60] R. Jackiw, *Lower Dimensional Gravity*, *Nucl. Phys. B* **252** (1985) 343–356.
- [61] C. Teitelboim, *Gravitation and Hamiltonian Structure in Two Space-Time Dimensions*, *Phys. Lett. B* **126** (1983) 41–45.
- [62] S. W. Hawking and D. N. Page, *Thermodynamics of Black Holes in anti-De Sitter Space*, *Commun. Math. Phys.* **87** (1983) 577.
- [63] M. Socolovsky, *Schwarzschild Black Hole in Anti-De Sitter Space*, *Adv. Appl. Clifford Algebras* **28** (2018) 18, [1711.02744].
- [64] L. Anderson, O. Parrikar and R. M. Soni, *Islands with Gravitating Baths: Towards ER = EPR*, 2103.14746.
- [65] J. Maldacena and L. Susskind, *Cool horizons for entangled black holes*, *Fortsch. Phys.* **61** (2013) 781–811, [1306.0533].
- [66] T. Banks and M. O’Loughlin, *Two-dimensional quantum gravity in Minkowski space*, *Nucl. Phys. B* **362** (1991) 649–664.
- [67] D. Louis-Martinez, J. Gegenberg and G. Kunstatter, *Exact dirac quantization of all 2d dilaton gravity theories*, *Physics Letters B* **321** (Jan, 1994) 193–198.

- [68] M. CAVAGLIÀ, *A note on weyl transformations in two-dimensional dilaton gravity*, *Modern Physics Letters A* **15** (Nov, 2000) 2113–2118.